UV-blocking spectacle lens protects against UV-induced decline of visual performance

Jyh-Cheng Liou,[1,2,4] Mei-Ching Teng,[3] Yun-Shan Tsai,[1,2] En-Chieh Lin,[1,2] Bo-Yie Chen[1,2]

[1]Department of Ophthalmology, Chung Shan Medical University Hospital, Taichung, Taiwan; [2]School of Optometry, Chung Shan Medical University, Taichung, Taiwan; [3]Department of Ophthalmology, Kaohsiung Chang Gung Memorial Hospital, Chang Gung University College of Medicine, Kaohsiung, Taiwan; [4]Institute of Medicine, Chung Shan Medical University, Taichung, Taiwan

Purpose: Excessive exposure to sunlight may be a risk factor for ocular diseases and reduced visual performance. This study was designed to examine the ability of an ultraviolet (UV)-blocking spectacle lens to prevent visual acuity decline and ocular surface disorders in a mouse model of UVB-induced photokeratitis.
Methods: Mice were divided into 4 groups (10 mice per group): (1) a blank control group (no exposure to UV radiation), (2) a UVB/no lens group (mice exposed to UVB rays, but without lens protection), (3) a UVB/UV400 group (mice exposed to UVB rays and protected using the CR-39™ spectacle lens [UV400 coating]), and (4) a UVB/photochromic group (mice exposed to UVB rays and protected using the CR-39™ spectacle lens [photochromic coating]). We investigated UVB-induced changes in visual acuity and in corneal smoothness, opacity, and lissamine green staining. We also evaluated the correlation between visual acuity decline and changes to the corneal surface parameters. Tissue sections were prepared and stained immunohistochemically to evaluate the structural integrity of the cornea and conjunctiva.
Results: In blank controls, the cornea remained undamaged, whereas in UVB-exposed mice, the corneal surface was disrupted; this disruption significantly correlated with a concomitant decline in visual acuity. Both the UVB/UV400 and UVB/photochromic groups had sharper visual acuity and a healthier corneal surface than the UVB/no lens group. Eyes in both protected groups also showed better corneal and conjunctival structural integrity than unprotected eyes. Furthermore, there were fewer apoptotic cells and less polymorphonuclear leukocyte infiltration in corneas protected by the spectacle lenses.
Conclusions: The model established herein reliably determines the protective effect of UV-blocking ophthalmic biomaterials, because the in vivo protection against UV-induced ocular damage and visual acuity decline was easily defined.

The anterior layers of the eye, particularly the cornea and conjunctiva, are important in ultraviolet (UV) light absorption. The physiologic effects of UV rays on these layers are strictly correlated with their wavelengths. Accordingly, the UV spectrum is subdivided into three classes: UVA (320–400 nm), UVB (290–320 nm), and UVC (200–290 nm) [1]. Studies have shown that UVB radiation confers a higher risk of ocular surface disease than does UVA [2,3]. UV radiation, especially UVB, plays a major role in the pathogenesis of both photokeratitis and photoconjunctivitis [2,3] through its ability to cause direct and indirect cellular damage. This involves a complex process of cell death, matrix remodeling, oxidative stress, and inflammation [4-7]. Therefore, there is great demand for novel and effective strategies aimed at reducing UV photodamage and associated visual health problems.

Several studies [8,9], as well as our previous laboratory experiments [5-7], have revealed that repeated irradiation of the mouse cornea using UVB radiation causes gradually worsening abnormality in the corneal tissue. This is accompanied by inflammation and the development of an irregular morphology, as well as by metabolic disturbances in the cornea. Under UVB irradiation, corneal damage is mediated through increased levels of lipid peroxidation products (malondialdehyde and 4-hydroxynonenal) [5,7,9], inflammatory mediators (NF-κB and COX-2) [5-7,10], cell death factors (Fas receptor) [6], and matrix metalloproteinases (MMP-9 and MMP-2) [7,11]. Studies have shown that certain natural antioxidants or therapeutics, such as zerumbone [5], α-lipoic acid [7], lornoxicam [10], and (-)-epigallocatechin-3-gallate (EGCG) [12], prevent UVB-induced corneal pathology and UV photodamage in the mouse cornea. This is because of their ability to combine oxidative stress reduction with the promotion of defense mechanisms by increasing the levels of endogenous antioxidant enzymes. Furthermore, UV-blocking soft contact lenses have been demonstrated to protect the cornea [6,9], crystalline lens [13,14], and retina [9] from UV photodamage in animal models. Specifically, in our own laboratory, certain beneficial effects on the cornea of UV-blocking soft contact lenses have been investigated in vivo using a mouse model of UVB keratitis [6]. Based on

Correspondence to: Bo-Yie Chen, School of Optometry, Chung Shan Medical University, No. 110, Chien-Kuo North Road, Taichung 402, Taiwan; Phone: +886-4-2473-0022 ext. 12319; FAX: +886-4-2324-8131; email: boychen@csmu.edu.tw

these previous experiments, we have used a 0.72 J/cm² daily dose of UVB for 7 days in the experiment presented herein.

A reflective film coating on spectacle lenses is known to provide numerous visual benefits to wearers [15,16]. However, spectacle lenses coated with UV-absorbing or UV-reflective monomers specifically reflect UV wavelengths, which lie outside the visible spectrum, so as to reduce UV transmittance to the eye. However, it is unclear whether these lenses protect corneal structures or visual performance. The present study provides clinical insights that have not been addressed in previous reports into protection of the visual system from UV wavelengths. The study examined the UV-blocking properties of two varieties of the CR-39™ spectacle lens: one with a UV400 coating and another with a photochromic coating (Transitions®). We used a mouse model involving UV-induced changes to the anterior eye and to visual function.

METHODS

Mouse model and experimental design: Female imprinting control region (ICR) mice (6 to 7 weeks) were purchased from the National Laboratory Animal Center, Taipei, Taiwan. All mice were examined using a dissecting microscope and slit lamp microscope before experiments. Only mice with normal ocular surfaces and visual acuity were included in the experiments. All procedures were approved by the Animal Care and Use Committee of Chung Shan Medical University and followed the ARVO guidelines for animal care and use. Ocular surface pathologies were induced using a UVB lamp (peak wavelength: 312 nm; power density: 8 mW/cm²; duration: 90 s, once daily, 7 days; total daily exposure: 0.72 J/cm²/day; CN-6, Vilber Lourmat, Germany) [5-7]. The experiment

was performed at the same time each day. The UVB wavelength ranged from 280 nm to 320 nm, with a peak at 312 nm. The mice were split into four groups: (1) a blank control group, where mice were not exposed to UVB; (2) a UVB/no lens group, where mice were exposed to UVB rays, but without spectacle lens protection; (3) a UVB/UV400 group, where mice were exposed to UVB rays and covered using the CR-39™ spectacle lens with UV400 coating (SMJ Holdings Pte. Ltd., Tainan, Taiwan); and (4) a UVB/photochromic group, where mice were exposed to UVB rays and covered using the CR-39™ spectacle lens with photochromic coating (Transitions®; SMJ Holdings Pte. Ltd., Tainan, Taiwan). To briefly describe the procedure, after general anesthesia, the mouse eyes in the relevant groups were covered using the CR-39™ spectacle lens and then exposed to UVB (Figure 1). The distance between the mouse cornea and UVB lamp was approximately 15 cm. After each daily UVB exposure, the mice in the exposed groups were allowed to recover for 15 min, during which saline eye drops were applied two to three times to avoid dryness on the eye surface. The mice were then treated topically with 1 μl of 0.4% ketorolac to reduce ocular pain. Each spectacle lens used in this study was repetitively exposed to UVB.

Mouse visual acuity analysis: In all the UVB-exposed groups, visual acuities were measured on Day 0 before UVB exposure (baseline) and on Day 7 after UVB exposure. Measurements were made using a modified optokinetic head-tracking response system [17-19], a behavioral measure of visual acuity. In the blank control group, the mouse visual acuities were measured on Day 0 (baseline) and on Day 7. Visual acuity was measured by single-blinded, independent observers.
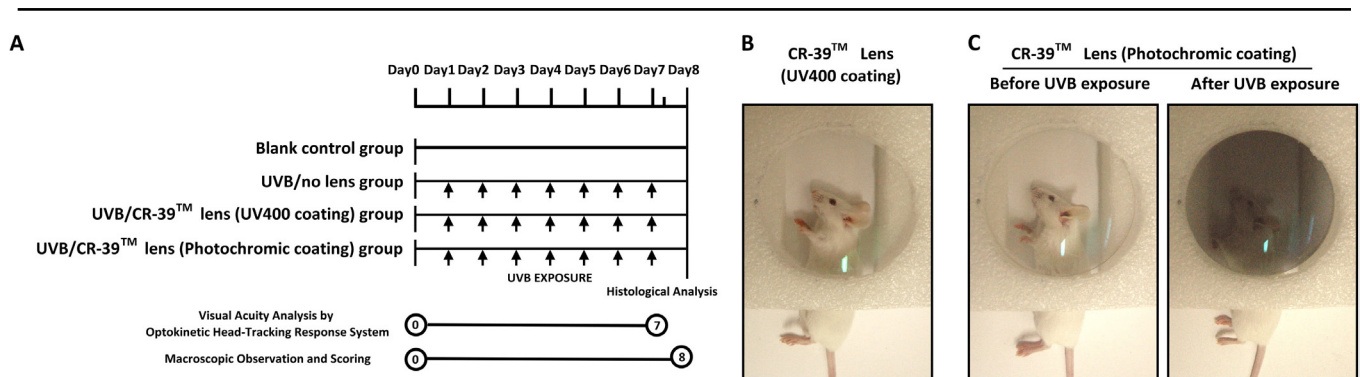

Figure 1. Experimental groups and experimental protocol for CR-39™ spectacle lens protection. **A:** Daily UVB light exposure (indicated by arrows) once daily to a total amount of 0.72J/cm² was performed from Day 1 to Day 7, with or without CR-39™ spectacle lenses. No lens was given to the UVB group or the blank control group. **B** and **C:** An actual experimental preparation of mouse eyes covered with CR-39™ spectacle lens was demonstrated. A representative mouse, after being anesthetized, covered by a CR-39™ lens with UV400 and photochromic coating, and was exposed to UVB.

Macroscopic observation, parameters, and scoring of corneal smoothness, opacity, and Lissamine green staining: All mice were anesthetized before assessment. Corneas were observed macroscopically and topographically on both Day 0 and Day 8. One eye from each mouse was randomly selected to assess corneal smoothness and opacity. This assessment was performed using a topographer that projects a single illuminated ring, followed by a series of illuminated rings, onto the corneal surface. After assessing corneal smoothness and opacity, the second eye from each mouse was subjected to corneal staining using 1 µl of 1% lissamine green (Sigma–Aldrich, St. Louis, MO). Images of the corneal surface were taken, and smoothness, opacity, and lissamine green staining were scored according to a graded scale of severity. The details of this scoring system have been published previously [5-7]. Briefly, corneal smoothness in all groups was scored as 0 (no distortion), 1 (distortion in one quadrant of the ring), 2 (distortion in two quadrants of the ring), 3 (distortion in three quadrants of the ring), 4 (distortion in all four quadrants of the ring), or 5 (severe distortion in which no ring was distinguishable). Corneal opacity was scored in all groups as 0 (normal cornea without haze), 1 (mild haze), 2 (moderate haze with visible iris), 3 (severe haze with invisible iris), 4 (severe haze with corneal ulceration), or 5 (severe haze with corneal ulceration and angiogenesis). Corneal lissamine green staining was scored as 0 (without punctuate staining), 1 (less than 20% of the corneal surface with scattered punctuate staining), 2 (20%–40% of the corneal surface with diffuse punctate staining), 3 (40%–60% of the corneal surface with diffuse punctate staining), 4 (60%–80% of the corneal surface with diffuse punctate staining), or 5 (more than 80% of the corneal surface with abundant staining) in all experimental groups. A total pathological change score was calculated by adding the three individual scores to give a result from 0 to 15. All scoring was performed by two observers who had no prior knowledge of UVB exposure or the study groups.

Histological analysis, immunohistochemistry, and TUNEL staining: All mice were euthanized by CO_2 inhalation 24 h after final UVB exposure on Day 8. The eyeballs were immersed in 4% formalin fixative overnight. After conventional paraffin embedding and histological section preparation, samples were examined using either hematoxylin-eosin or periodic acid Schiff (PAS) staining [5-7]. The thickness of the outer nuclear layer (ONL) was measured parallel to the vertical meridian of the eye at a distance of 1 mm from the optic nerve head. For immunohistochemistry, tissue sections were boiled in a citrate buffer (pH 6.0) to retrieve the antigen and then subjected to standard procedures of antibody incubation and color detection, as well as counterstaining using hematoxylin. The primary antibodies used in this study were anti-MMP-9 (1/100 dilution, NB110–89719), anti-CK5 (1/600 dilution, NBP1–67613), and anti-Fas (1/100 dilution, NBP1–41407), which were purchased from Novus Biologicals (Littleton, CO), and anti-P63 (1/50 dilution, sc-8431), which was purchased from Santa Cruz Biotechnology (Santa Cruz, CA). To measure end-stage apoptosis, a terminal deoxynucleotidyl transferase dUTP nick end labeling (TUNEL) assay was performed using the ApoBrdU-IHC DNA Fragmentation Assay Kit (BioVision) according to the manufacturer's instructions.

Statistical analysis: All data were obtained from eight individual mouse corneas. Statistics were analyzed using the SPSS program (SPSS, Inc., Chicago, IL), and graphs were generated using Microsoft Excel 2010. The data obtained from all groups were analyzed using the Kruskal–Wallis nonparametric ANOVA, and the Mann–Whitney U-test for pairwise comparisons in cases when the Kruskal–Wallis test was significant. The data obtained on Day 7 were compared with the baseline measurements using a paired *t*-test. The results were considered statistically significant at $p<0.001$. The correlation between visual acuity decline and changes to the corneal surface was assessed using Pearson's correlation test. The results were considered significant at $p<0.05$.

RESULTS

Effects of spectacle lens with anti-UV coating on the ocular surface protection after UVB exposure: Macroscopically, none of the control mice had evidence of disorders on the corneal surface. The healthy cornea under topographical analysis showed a smooth white-light ring reflecting off the cornea (Figure 2A), a regular topographic pattern (Figure 2E), a transparent corneal surface (Figure 2I), and no lissamine green staining (Figure 2M). By comparison, the corneas of the UVB/no lens group showed less smoothness (Figure 2B), an irregular topographic pattern (Figure 2F), severe corneal opacification, edema (Figure 2J), and large dark blue devitalized epithelial areas (Figure 2N). After UVB exposure, the pathological changes to the mouse corneal surface were similar to our previous reports [5-7]. By contrast, the corneas of both the UVB/UV400 (Figure 2C,G,K,O) and UVB/photochromic groups (Figure 2D,H,L,P) were normal, without evidence of disorders on the surface.

The differences among the experimental groups regarding the corneal smoothness score (Figure 2Q), corneal opacity score (Figure 2R), and corneal lissamine green staining score (Figure 2S) were analyzed quantitatively. In the UVB/no lens group, the mean corneal surface disorder scores were significantly higher than those of the other groups
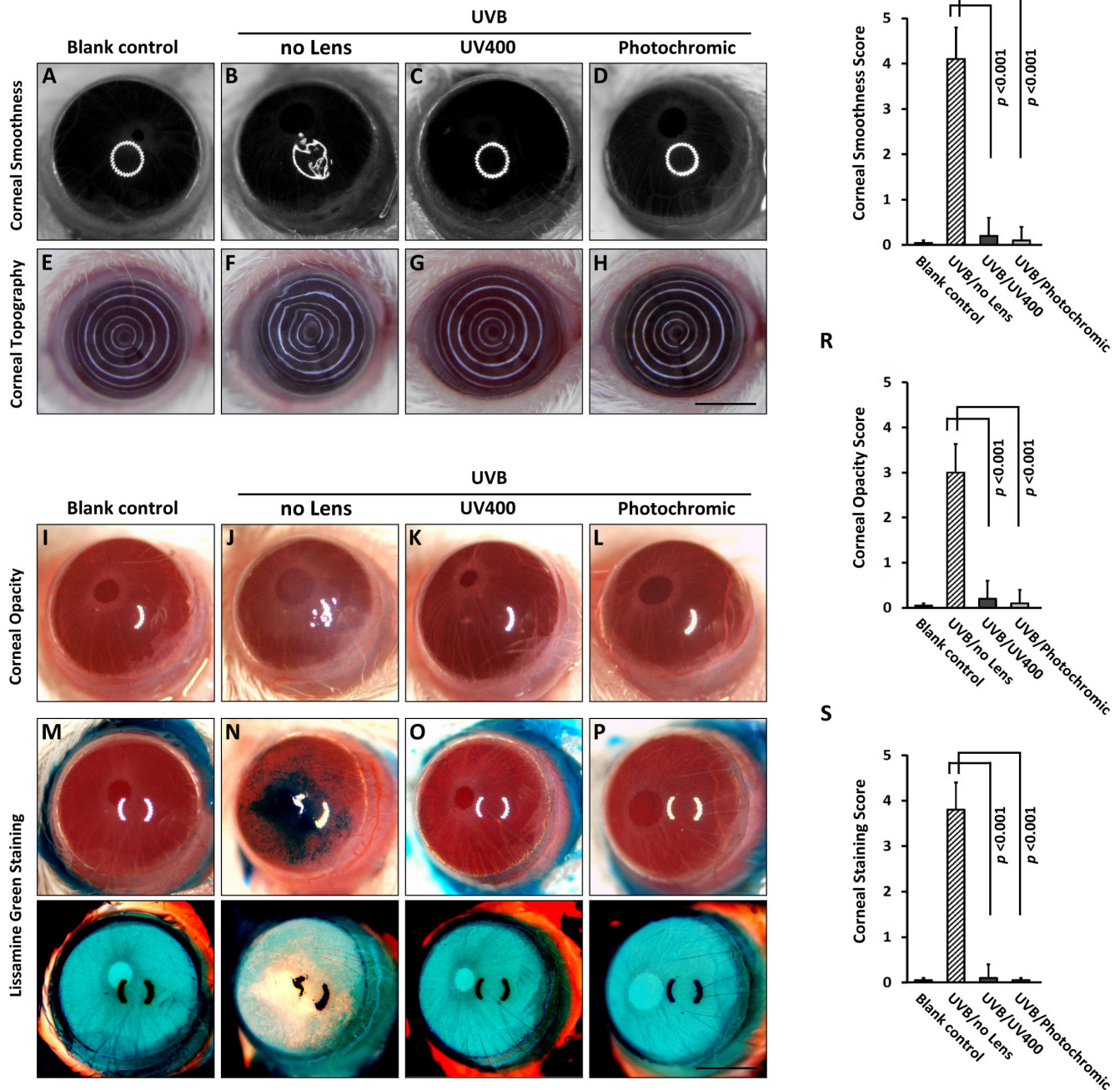
Figure 2. Representative photos for corneal surface evaluation among the experimental groups after daily treatments of UVR ($0.72 J/cm^2$/ daily) for a period of 7 days. **A-D**: The corneal smoothness. **E-H**: The corneal topography. **I- L**: the corneal opacity and **M-P**: the corneal lissamine green staining among the four study groups were assessed as parameters for the in vivo UVB protective properties. The photos in the bottom row of **M**, **N**, **O**, and **P** are the corresponding negative images. **Q**, **R**, and **S**: Quantitative analyses (n = 10 per group) were also performed. The results show that all scores were reduced with the shield protective effects from spectacle lens. All scale bars: 1.25 mm.
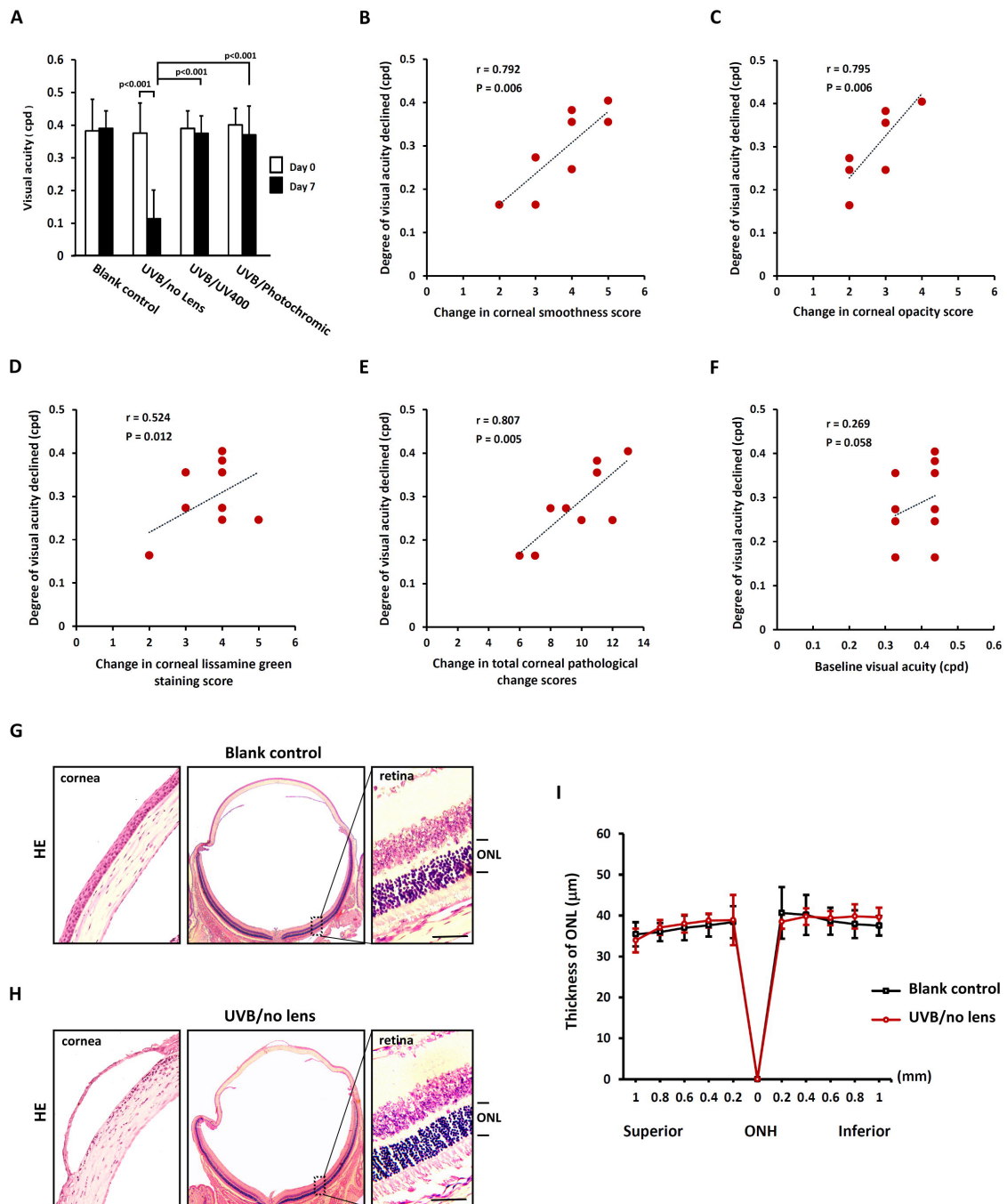
Figure 3. The benefit of both CR-39™ spectacle lenses in visual performance against UV radiation. **A:** The UV-induced decline in visual acuity was significantly prevented by CR-39™ spectacle lens protection. **B**, **C**, and **D:** Scatterplots demonstrating the relationship between the changes in corneal smoothness, corneal opacity, and corneal lissamine green staining scores and the reduced degrees of visual acuity after UVB exposure. **E** and **F:** Scatterplots demonstrating the relationship between the changes in total corneal pathological changes scores, and baseline visual acuity and the reduced degrees of visual acuity after UVB exposure. **G:** HE staining showing the normal cornea and retina of the blank control mouse. **H:** HE staining showing severe damage in the corneal tissue of the unprotected mouse, in which no evidence of histological abnormality was found in the retinal photoreceptor. **I:** The outer nuclear layer thickness for UVB-exposed and blank control mice was valued. Values were mean±SD (n=6, each group). There were no statistically significant differences between the two groups at any distance point. ONL: outer nucleus layer. ONH: optic nerve head. Scale bars: 35 mm.

(p<0.001). Particularly, no abnormal corneas were evident in either of the CR-39™ spectacle lens groups.

Effects of spectacle lens with anti-UV coating on visual performance after UVB exposure: None of the control mice (non-UVB exposed) had evidence of vision problems, as measured by the optokinetic head-tracking response system, a behavioral measure of visual acuity. On the other hand, visual acuity in the UVB/no lens group had declined significantly on Day 7 after UVB exposure (0.107±0.049 cycles per degree [cpd]) from baseline (0.393±0.053 CPD; p<0.001; Figure 3A).

Conversely, the visual acuity values in both the UVB/UV400 (0.389±0.054 cpd) and UVB/photochromic groups (0.387±0.084 cpd) were similar to the baseline level (0.401±0.052 and 0.407±0.049 cpd, respectively) at the end of Day 7 (Figure 3A). As a comparison, the mean visual acuities in the control group were 0.392±0.097 cpd at baseline and 0.390±0.054 cpd at the end of Day 7. Significant differences were found among the UVB/no lens, UVB/UV400, and UVB/photochromic groups with regard to visual acuity scores on Day 7 (p<0.001), but not between the UVB/UV400 and UVB/photochromic groups (Figure 3A). Taken together, we surmise that the unprotected corneas of mice in the UVB/no lens group exhibited different levels of visual acuity decline precisely because of the different degrees of pathological change on the corneal surface.

Decline in visual performance is correlated with the progress of corneal pathological changes after UVB exposure: The visual acuity of the unprotected group declined significantly, from 0.393±0.053 cpd at baseline to 0.107±0.049 cpd after UVB exposure (p<0.001). The decrease during the study period was 0.286±0.081 cpd. We therefore analyzed the correlation between this reduced visual acuity and the aforementioned corneal pathological changes; that is, corneal smoothness, opacity, and lissamine green staining. Only the data from the UVB/no lens group were analyzed in this regard. After UVB exposure, the visual acuity decline showed significant simple correlation with the changes in all three scores: the corneal smoothness score (Pearson's correlation coefficient; r=0.792, p=0.006; Figure 3B), the corneal opacity score (r=0.795, p=0.006; Figure 3C), and the corneal lissamine green staining score (r=0.524, p=0.012; Figure 3D). Moreover, visual acuity decline was significantly correlated with the total pathological change score (r=0.807, p=0.005; Figure 3E), but not with the baseline visual acuity (r=0.269, p=0.058; Figure 3F).

Lens opacity or loss of retinal cells would also contribute to a decline in visual performance. At the end of the experiment, the changes in lens transparency in the UVB-exposed eyes were too mild to be visualized using slit lamp examination. Microscopically, the retinal tissues in the UVB-exposed eyes were normal—no severe degeneration of the retinal photoreceptors occurred (Figure 3G,H). Furthermore, there were no significant differences between the blank control and UVB/no lens groups with regard to the thickness of the retinal ONL (Figure 3I). Thus, the UVB-induced corneal pathological changes in mice may be the predominant influencing factor in visual acuity decline, and this resulted in the significant correlation seen.

Spectacle lens with anti-UV coating protected against the UVB-induced degeneration of ocular surface: Microscopically, no evidence of histological abnormality was found in the corneal tissue from the control (Figure 4A), UVB/UV400 (Figure 4C), and UVB/photochromic groups (Figure 4D). In contrast, the cornea from the UVB/no lens group revealed severe lesions, with thin corneal epithelium, friable edematous stroma (Figure 4B), and polymorphonuclear (PMN) leukocyte infiltration (Figure 4B; indicated by arrow). The infiltrative PMN leukocytes in the corneal lesions may produce certain proteolytic enzymes; indeed, MMP-9 was found on the corneal surface using immunohistochemistry (Figure 4F). These enzymes may not only degrade the extracellular matrix molecules in the stroma, but also destroy the structural integrity of the epithelium with varying degrees of severity. On the other hand, no evidence of the MMP-9 protein was detected in the corneal tissue of the control (Figure 4E), UVB/UV400 (Figure 4G), and UVB/photochromic groups (Figure 4H). The differences among the groups with regard to corneal epithelial thickness (Figure 4I) and PMN leukocyte counts (Figure 4J) were analyzed using quantitative analysis (p<0.001).

Corneal surface layer epithelium is a self-renewing tissue that contains P63+ basal cells (Figure 4K) and CK-5+ epithelial cells (Figure 4O). Consistent with our previous reports [5-7], in the unprotected cornea after UVB exposure, the surface CK-5+ epithelium had been thinned to three or four layers (Figure 4P); and P63+ basal cells with regeneration capacity became scarce (Figure 4L). Conversely, upon UVB irradiation, the degeneration of P63+ basal cells and CK-5+ epithelium was significantly suppressed in the corneas of both the UVB/UV400 (Figure 4M,Q) and UVB/photochromic groups (Figure 4N,R). In addition, we compared apoptotic cell counts in the corneas among the experimental groups using TUNEL labeling. More TUNEL-positive cells were detected in the corneal lesions (Figure 4T) of the unprotected cornea than in those of the 2 spectacle lens-protected groups (Figure 4U,V) after UVB exposure. There were no apoptotic cells detected in corneas of the control group (Figure 4S). It
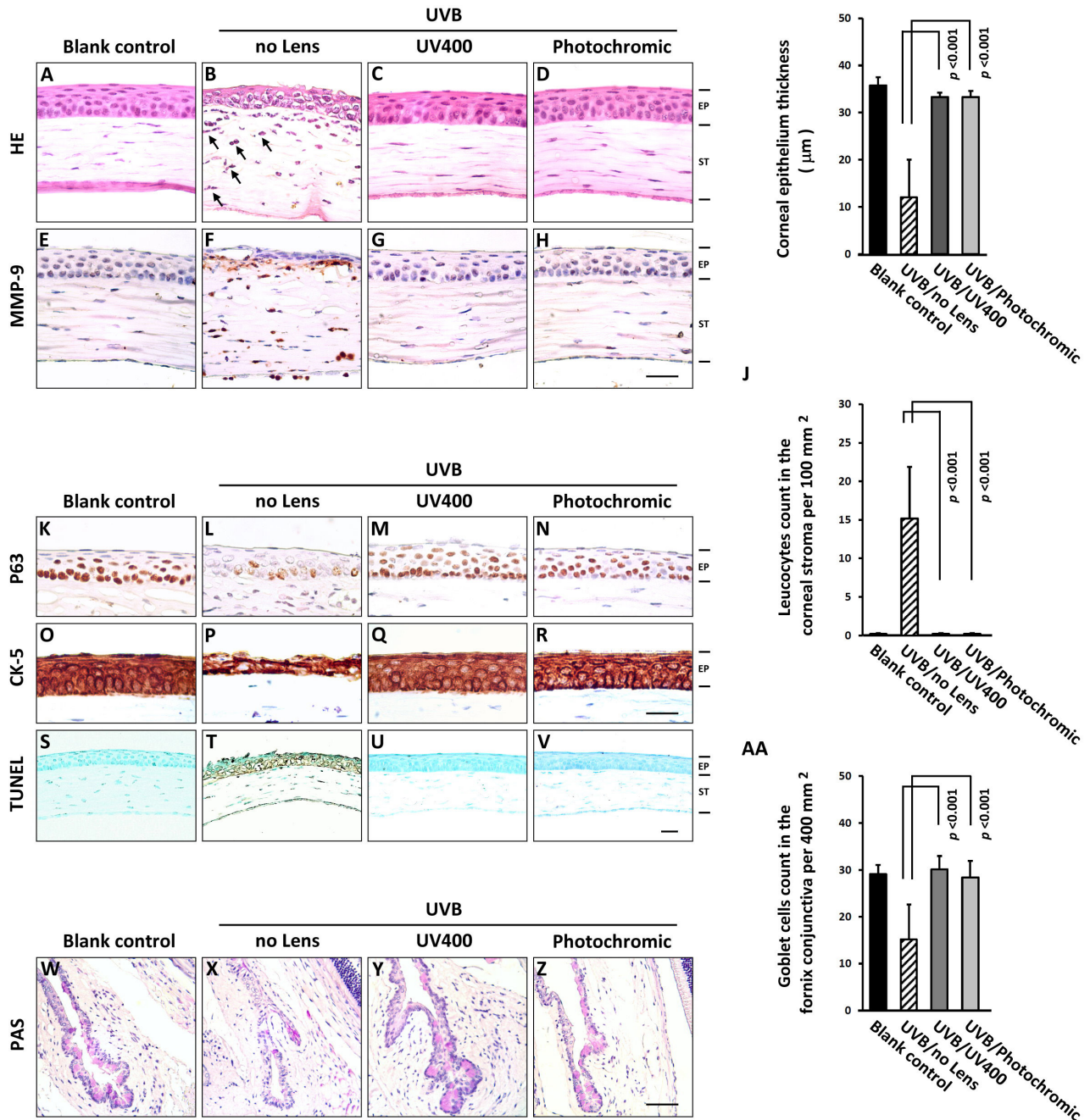
Figure 4. UV-blocking spectacle lens ameliorate UVB-induced damage of ocular surface and inflammation. **A-H**: Histological analysis showing disordered corneal surface structure and inflammation in the unprotected cornea, but not in the CR-39™ spectacle lens-protected cornea. The polymorphonuclear (PMN) leukocyte infiltration were found in the stromal layer (indicated by arrow in **B**). Quantitative analyses of the corneal epithelium thickness in **I** and polymorphonuclear leukocytes infiltration in **J** among the study group (n = 8 per group). **K-V**: Immunostaining showing evident inhibition of UV-induced loss of corneal cells (P63+ basal cells and CK-5+ epithelial cells) and UV-induced apoptosis by CR-39™ spectacle lens protection. **W-Z**: PAS staining showing that the UV-induced reduction of conjunctival goblet cells was significantly prevented by CR-39™ spectacle lens protection. **AA**: Quantitative analyses of goblet cells within the fornix conjunctival epithelium among the study group (n = 8 per group). EP: corneal epithelium. ST: corneal stroma. All scale bars: 25 µm.

follows that both spectacle lenses had a significant protective effect.

Next, the conjunctival epithelium was examined using PSA staining. In addition to the previous findings, fewer conjunctival goblet cells (pink color) were observed in the UVB/no lens group (Figure 4X) after UVB exposure. However, abundant goblet cells occurred in the conjunctival epithelia of the UVB/UV400 (Figure 4Y) and UVB/photochromic groups (Figure 4Z), as well as in the control group (Figure 4W). The differences among the experimental groups with regard to goblet cell count analyzed quantitatively (P < 0.001; Figure 4AA). Both types of CR-39™ spectacle lens with anti-UV coating significantly protected the corneal and conjunctival epithelia from UVB-induced cell death and degeneration.

DISCUSSION

UV phototoxicity is important in the processes associated with pathological changes to the ocular tissue. The risks of excess ocular tissue exposure to UV are well recognized, but the requirement for eye protection is frequently overlooked. Furthermore, the specific physiologic effects on vision in vivo of UV-blocking spectacle lenses or sunglasses are not well understood, despite the fact that such lenses are widely recommended. The human and mouse corneas absorb most 300 nm wavelength UVB [20,21], and although the UV transmittance of spectacle lenses, such as the CR-39™, has been confirmed using physical spectrophotometric methods, most coatings reflect UV radiation at unacceptably high levels [15,22]. Specifically, these lenses absorb all UVB and at least 99% of UVA [22].

However, the benefits of coating the CR-39™ using either UV400 or a photochromic coating (Transitions®) have not yet been elucidated. Particularly, the extent of improvement to visual performance, as well as to the prevention of UV-induced ocular damage, is not known. The present study showed a correlation between visual acuity decline and UV-induced corneal pathological changes in a mouse model, and indicated that mice that were irradiated using UVB and protected using the CR-39™ spectacle lens with anti-UV coatings maintained better visual acuity than unprotected mice.

Even though UVB irradiation is known to cause corneal damage in this mouse model [5-7], the influence of several UV-induced corneal pathological changes on visual acuity decline had not been previously reported. Reduced visual acuity can be clinically attributable to retinopathy, cataract, and corneal haze, as well as to certain corneal surface changes. The results here showed that, in UVB-exposed mice, changes in corneal smoothness, opacity, and lissamine green staining were significantly correlated with reduced visual acuity (Figure 3B-D). Furthermore, the progress of overall UV-induced corneal pathological change was significantly correlated with visual acuity decline (Figure 3E). By way of comparison, the visual acuities of mice in the two anti-UV-coated CR-39™ spectacle lens groups (UV400 and photochromic-coated lenses) were better-protected during UVB irradiation. The visual acuity in both these groups remained at the baseline level after UVB exposure (Figure 3A). Moreover, no evidence of abnormal changes on the cornea was found in these protected groups after UVB exposure (Figure 2). Our results suggest that the prevention of UV-induced damage and the protection of visual acuity in both types of CR-39™ spectacle lens is mediated by the UV reflective coating, since protection against UV-induced pathological changes on the cornea and vision in vivo was observed.

As we have previously shown, contact lenses with UV-blocking substrates may protect against UV irradiation-dependent thin epithelialization, stromal inflammation, and altered structural integrity in the mouse cornea [6]. The effect of UV irradiation-dependent oxidative stress on the unprotected cornea has also been investigated. Specifically, reactive oxygen species (ROS) levels and lipid peroxidation were significantly higher, whereas the antioxidant capacity was significantly lower, in unprotected mouse cornea after UVB exposure than in corneas protected using UV-blocking contact lenses [6,9]. Similarly, both antioxidant capacity and ascorbic acid levels in the aqueous humor have been found to be significantly lower in unprotected rabbit cornea after UVB exposure than in rabbit cornea protected using UV-blocking contact lenses [13]. Furthermore, oxidative stress has been suggested to activate certain pathological pathways that lead to progressive corneal thinning, apoptosis, and tissue degeneration, three major hallmarks of corneal photodamage. Also, UV cell-death induction in corneal epithelial cells has been visualized using transmission electron microscopy [10,13], and the mediators of such cell death in the UV-exposed cornea have been shown through immunohistochemistry to be NF-κB and COX-2 [5-7,10]. UV-blocking contact lenses have been demonstrated to significantly decrease cell death in the cornea in both rabbit [13] and mouse models [6,9]. It is likely that UV-blocking tints in the CR-39™ spectacle lens (such as the UV400- and photochromic-coated lenses used in the present study) would yield an even more significant difference in ocular surface protection. As evidence for this, corneal structural integrity was better preserved and more goblet cells occurred in the conjunctival epithelium in both

CR-39™ spectacle lens treatment groups than in the unprotected cornea (Figure 4E).

The production and activity of MMPs on the ocular surface have been found in patients with ocular surface inflammation [23,24]. In addition, the UV induction of MMPs like MMP-9 or MMP-2 can destroy the corneal basement membrane and cause pathological degradation of stromal collagen and proteoglycans [25,26]. UV blocking has been shown to attenuate the UV-induced production of MMPs by the corneal tissue in rabbit [11]; and the present study has now shown the same phenomenon in mouse. On the basis of these findings, it follows that UV-induced MMP production and activation initiate proteolytic activity, and contribute to pathological changes on the corneal surface. Such changes include roughness (Figure 2B) and opacification (Figure 2J). Additionally, inflammatory cells recruited to corneas by inflammation (Figure 4B,F) are thought to affect keratitis, which undoubtedly sustains and amplifies MMP activity [11]. The pathological effect of UV-induced inflammation and MMP production in the mouse conjunctival epithelium were not analyzed in the present study.

The clinical condition pterygium is an inflammatory and UV-related lesion on the ocular surface. In the current study, we think that MMPs contributed to pterygium pathogenesis [27-29], degradation of conjunctival or corneal tissue [28,29], and the role of UV induction of MMPs from ocular surface cells [29,30]. For this reason, ocular protection from solar UV radiation has been emphasized to avoid excess oxidative stress- or MMP-mediated tissue degeneration processes within the ocular tissue.

The daily dose of UVB used in this study (0.72 J/cm^2) approaches the reported threshold for developing corneal photokeratitis, cataract, and photoconjunctivitis after a seven-day application [5-7,31]. Zigman et al. reported that the average dose of solar UVB radiation is 0.105 J/cm^2 during a 1-h exposure of the human cornea [32]. Thus, the daily UVB dose used in this animal study was equivalent to exposing the human cornea to approximately 6 to 7 h of sunlight in only 90 s. Although the UVB dose used in this study was substantial, severely devitalized epithelial damage and irregular topographic pattern on the cornea were not noted in any of the spectacle-lens protected eyes. Furthermore, although declining visual acuity developed during the UVB exposure process in the unprotected treatment group, neither changes in retinal thickness nor photoreceptor loss were seen in the present study (Figure 3C).

The different levels of reduced visual acuity obtained after UVB exposure (Figure 3A) were due to, and have high correlation with, UV-induced pathological changes in the mouse cornea. UVB irradiation, together with corneal roughness, opacification, edema, and epithelial damage, may attenuate the light transmitted along the optic axis of the eye, leading to reduced visual acuity. Alternatively, UV-induced lens opacity would also contribute to a decline in visual performance. Nevertheless, under the present experimental conditions, the changes in lens transparency in the UVB-exposed eyes were too mild to be visualized by slit lamp examination. It has been postulated that the mouse iris muscles absorb the redundant UVB rays from the cornea, thus minimizing the absorptive effects of crystalline lens. However, previous reports have indicated that, following pupillary dilation with tropicamide, UVB can induce more obvious photochemical damage to the crystalline lens [31,33].

The experiments outlined in this study support our initial hypothesis: eyes that have been protected from UVB using UV-blocking spectacle lenses would yield similar results to those that have not been exposed to UVB—specifically that both corneal and conjunctival pathology would be similar, and that visual performance would be comparable among the groups. This conclusion is supported by data from the present study, as well as other recent studies. The data demonstrate that the CR-39™ spectacle lens, with either UV400 or photochromic coating (Transitions®), can minimize UV-induced ocular damage and prevent UV-induced decline in visual acuity. The findings strongly suggest that a UV-reflective sun spectacle lens should be tested using similar approaches in a bio-physiologic system. Determinant parameters of ocular surface bio-physiology should be evaluated to confirm that eyewear with spectacle lenses can prevent UV radiation from reaching the eye in vivo, even if the UV transmittance of the spectacle lens has been measured using physical spectrophotometric methods.

REFERENCES

1. Chandler H. Ultraviolet absorption by contact lenses and the significance on the ocular anterior segment. Eye Contact Lens 2011; 37:259-66. [PMID: 21646978].

2. Taylor HR. The biological effects of UV-B on the eye. Photochem Photobiol 1989; 50:489-92. [PMID: 2687903].

3. Wang F, Gao Q, Hu L, Gao N, Ge T, Yu J, Liu Y. Risk of eye damage from the wavelength-dependent biologically effective UVB spectrum irradiances. PLoS ONE 2012; 7:e52259- [PMID: 23284960].

4. Jauhonen HM, Kauppinen A, Paimela T, Laihia JK, Leino L, Salminen A Kaarniranta K. Cis-urocanic acid inhibits SAPK/JNK signaling pathway in UV-B exposed human corneal epithelial cells in vitro. Mol Vis 2011; 17:2311-7. [PMID: 21921982].

5. Chen BY, Lin DP, Wu CY, Teng MC, Sun CY, Tsai YT, Su KC, Wang SR, Chang HH. Dietary zerumbone prevents mouse cornea from UVB-induced photokeratitis through inhibition of NF-kappaB, iNOS, and TNF-alpha expression and reduction of MDA accumulation. Mol Vis 2011; 17:854-63. [PMID: 21527993].

6. Lin DP, Chang HH, Yang LC, Huang TP, Liu HJ, Chang LS, Lin CH, Chen BY. Assessment of ultraviolet B-blocking effects of weekly disposable contact lenses on corneal surface in a mouse model. Mol Vis 2013; 19:1158-68. [PMID: 23734085].

7. Chen BY, Lin DP, Chang LS, Huang TP, Liu HJ, Luk CP, Lo YL, Chang HH. Dietary alpha-lipoic acid prevents UVB-induced corneal and conjunctival degeneration through multiple effects. Invest Ophthalmol Vis Sci 2013; 54:6757-66. [PMID: 23989186].

8. Newkirk KM, Chandler HL, Parent AE, Young DC, Colitz CM, Wilkie DA, Kusewitt DF. Ultraviolet radiation-induced corneal degeneration in 129 mice. Toxicol Pathol 2007; 35:819-26. [PMID: 17943656].

9. Ibrahim OM, Kojima T, Wakamatsu TH, Dogru M, Matsumoto Y, Ogawa Y, Ogawa J, Negishi K, Shimazaki J, Sakamoto Y, Sasaki H, Tsubota K. Corneal and retinal effects of ultraviolet-B exposure in a soft contact lens mouse model. Invest Ophthalmol Vis Sci 2012; 53:2403-13. [PMID: 22410564].

10. Yin J, Huang Z, Wu B, Shi Y, Cao C, Lu Y. Lornoxicam protects mouse cornea from UVB-induced damage via inhibition of NF-{kappa}B activation. Br J Ophthalmol 2008; 92:562-8. [PMID: 18369073].

11. Chandler HL, Reuter KS, Sinnott LT, Nichols JJ. Prevention of UV-induced damage to the anterior segment using class I UV-absorbing hydrogel contact lenses. Invest Ophthalmol Vis Sci 2010; 51:172-8. [PMID: 19710408].

12. Chen MH, Tsai CF, Hsu YW, Lu FJ. Epigallocatechin gallate eye drops protect against ultraviolet B-induced corneal oxidative damage in mice. Mol Vis 2014; 20:153-62. [PMID: 24520184].

13. Giblin FJ, Lin LR, Leverenz VR, Dang L. A class I (Senofilcon A) soft contact lens prevents UVB-induced ocular effects, including cataract, in the rabbit in vivo. Invest Ophthalmol Vis Sci 2011; 52:3667-75. [PMID: 21421866].

14. Giblin FJ, Lin LR, Simpanya MF, Leverenz VR, Fick CE. A Class I UV-blocking (senofilcon A) soft contact lens prevents UVA-induced yellow fluorescence and NADH loss in the rabbit lens nucleus in vivo. Exp Eye Res 2012; 102:17-27. [PMID: 22766154].

15. Citek K. Anti-reflective coatings reflect ultraviolet radiation. Optometry 2008; 79:143-8. [PMID: 18302957].

16. Bachman WG, Weaver JL. Comparison between anti-reflection-coated and uncoated spectacle lenses for presbyopic highway patrol troopers. J Am Optom Assoc 1999; 70:103-9. [PMID: 10457687].

17. Prusky GT, Alam NM, Beekman S, Douglas RM. Rapid quantification of adult and developing mouse spatial vision using a virtual optomotor system. Invest Ophthalmol Vis Sci 2004; 45:4611-6. [PMID: 15557474].

18. Douglas RM, Alam NM, Silver BD, McGill TJ, Tschetter WW, Prusky GT. Independent visual threshold measurements in the two eyes of freely moving rats and mice using a virtual-reality optokinetic system. Vis Neurosci 2005; 22:677-84. [PMID: 16332278].

19. Pearson RA, Barber AC, Rizzi M, Hippert C, Xue T, West EL, Duran Y, Smith AJ, Chuang JZ, Azam SA, Luhmann UF, Benucci A, Sung CH, Bainbridge JW, Carandini M, Yau KW, Sowden JC, Ali RR. Restoration of vision after transplantation of photoreceptors. Nature 2012; 485:99-103. [PMID: 22522934].

20. Lembares A, Hu XH, Kalmus GW. Absorption spectra of corneas in the far ultraviolet region. Invest Ophthalmol Vis Sci 1997; 38:1283-7. [PMID: 9152249].

21. Dillon J, Zheng L, Merriam JC, Gaillard ER. The optical properties of the anterior segment of the eye: implications for cortical cataract. Exp Eye Res 1999; 68:785-95. [PMID: 10375442].

22. Lee DY, Brown WL, Trachimowicz R. Efficacy and durability of ultraviolet tints in CR-39 ophthalmic lenses. J Am Optom Assoc 1997; 68:709-14. [PMID: 9409106].

23. Acera A, Rocha G, Vecino E, Lema I, Duran JA. Inflammatory markers in the tears of patients with ocular surface disease. Ophthalmic Res 2008; 40:315-21. [PMID: 18688174].

24. Singh A, Maurya OP, Jagannadhan MV, Patel A. Matrix metalloproteinases (MMP-2 and MMP-9) activity in corneal ulcer and ocular surface disorders determined by gelatin zymography. J Ocul Biol Dis Infor 2012; 5:31-5. [PMID: 24376903].

25. Li DQ, Pflugfelder SC. Matrix metalloproteinases in corneal inflammation. Ocul Surf 2005; 3:SupplS198-202. [PMID: 17216119].

26. Kato T, Saika S, Ohnishi Y. Effects of the matrix metalloproteinase inhibitor GM6001 on the destruction and alteration of epithelial basement membrane during the healing of post-alkali burn in rabbit cornea. Jpn J Ophthalmol 2006; 50:90-5. [PMID: 16604381].

27. Schellini SA, Hoyama E, Oliveira DE, Bacchi CE, Padovani CR. Matrix metalloproteinase-9 expression in pterygium. Arq Bras Oftalmol 2006; 69:161-4. [PMID: 16699663].

28. Tsai YY, Chiang CC, Yeh KT, Lee H, Cheng YW. Effect of TIMP-1 and MMP in pterygium invasion. Invest Ophthalmol Vis Sci 2010; 51:3462-7. [PMID: 20207965].

29. Ng J, Coroneo MT, Wakefield D, Di Girolamo N. Ultraviolet radiation and the role of matrix metalloproteinases in the pathogenesis of ocular surface squamous neoplasia. Invest Ophthalmol Vis Sci 2008; 49:5295-306. [PMID: 18641285].

30. Di Girolamo N, Coroneo MT, Wakefield D. UVB-elicited induction of MMP-1 expression in human ocular surface epithelial cells is mediated through the ERK1/2 MAPK-dependent pathway. Invest Ophthalmol Vis Sci 2003; 44:4705-14. [PMID: 14578390].

31. Chen BY, Lin DP, Su KC, Chen YL, Wu CY, Teng MC, Tsai YT, Sun CY, Wang SR, Chang HH. Dietary zerumbone prevents against ultraviolet B-induced cataractogenesis in the mouse. Mol Vis 2011; 17:723-30. [PMID: 21423870].

32. Zigman S. Environmental near-UV radiation and cataracts. Optom Vis Sci 1995; 72:899-901. [PMID: 8749337].

33. Meyer LM, Söderberg P, Dong X, Wegener A. UVR-B induced cataract development in C57 mice. Exp Eye Res 2005; 81:389-94. [PMID: 16185949].